ÖZGÜN ARAŞTIRMA ORIGINAL RESEARCH

Med J SDU / SDÜ Tıp Fak Derg ▶ 2022:29(1):111-120 doi: 10.17343/sdutfd.1016353

SURFACE MODIFIED TITANIUM DIOXIDE/POLY (LACTIC ACID) NANOCOMPOSITE FILMS FOR TISSUE ENGINEERING

DOKU MÜHENDİSLİĞİ İÇİN YÜZEYİ MODİFİYE EDİLMİŞ TİTANYUM DİOKSİT/POLİ (LAKTİK ASİT) NANOKOMPOZİT FİLMLER

Ş. Melda ESKITOROS-TOGAY[1,2], Ulya TOKGÖZ[2]

[1] University of Health Sciences, Gulhane Vocational School of Health Services, Department of Pharmacy Services, Ankara, TURKEY

[2] Gazi University, Faculty of Engineering, Department of Chemical Engineering, Ankara, TURKEY

Cite this article as: Eskitoros-Togay ŞM, Tokgöz U. Surface Modified Titanium Dioxide/Poly(Lactic Acid) Nanocomposite Films for Tissue Engineering. Med J SDU 2022; 29(1): 111-120.

Öz

Amaç

Bu çalışmanın amacı, poli(laktik asit) matrisi içerisinde modifiye edilmemiş ve modifiye edilmiş nanopartiküller içeren nanokompozit filmleri sentezlemek, karakterize etmek ve doku mühendisliğinde alternatif bir yapı iskelesi olarak kullanımlarını araştırmaktır.

Gereç ve Yöntem

İlk olarak, titanyum dioksit (TiO_2) nanopartikülleri sırasıyla L-laktik asit oligomeri (LA-g-TiO_2) ve propiyonik asit/heksilamin (AA-g-TiO_2) karışımı ile aşılanmıştır. Daha sonra, PLA/TiO_2, PLA/LA-g-TiO_2 ve PLA/AA-g-TiO_2 nanokompozit filmleri üretmek için modifiye edilmemiş ve modifiye edilmiş nanopartiküller solvent döküm yöntemi ile poli (laktik asit) matrisi içine eklenmiştir. Sentezlenen bu filmlerin kimyasal, termal ve mekanik yapıları daha sonra karakterize edilmiştir.

Bulgular

Azaltılmış toplam yansıma (ATR) sonuçları, nanopartiküllerin yüzey modifikasyonunun başarılı olduğunu göstermiştir. Diferansiyel tarama kalorimetresi (DSC) analizinin sonuçları, modifiye edilmiş nanopartiküllerin dahil edilmesiyle PLA'nın kristalleşmesinin kısmen arttığını göstermiştir. Termogravimetrik analizin (TGA) sonuçları, polimer matrisine LA-g-TiO_2 eklenmesinin, PLA/LA-g-TiO_2 nanokompozit filmin termal stabilitesini, polimer matrisine AA-g-TiO_2 ilavesinden daha fazla geliştirdiğini göstermiştir. LA-g-TiO_2 içeren nanokompozitlerin birinci ve ikinci bozunma sıcaklıkları sırasıyla 348.3 °C ve 392 °C, saf PLA'nınkinden %6 daha yüksektir. Nanokompozitlerin atomik kuvvet mikroskobu (AFM) mikrografı, LA-g-TiO_2 ve AA-g-TiO_2 nanopartiküllerin polimer matrislerde homojen olarak dağıldığını göstermiştir. Dinamik mekanik analiz (DMA) sonuçları, diğer nanokompozitlere kıyasla PLA/LA-g-TiO_2 nanokompozitinde en verimli bağlanma ve uyumluluğun elde edildiğini göstermiştir.

Sonuç

Aşılanmış nanopartiküller, LA-g-TiO_2 ve AA-g-TiO_2, matris içindeki homojen dağılımları ve polimerik matris ile iyi etkileşimleri sayesinde nanokompozitlerin termal ve mekanik özelliklerini iyileştirmiştir. Bu nedenle, bu nanokompozitler kemik doku mühendisliğinde alternatif doku iskeleleri olarak kullanılabilir.

Anahtar Kelimeler: Poli(laktik asit), Yüzeyi modifiye edilmiş titanium dioksit, Aşılama, Nanokomposit, Nanopartikül, Doku mühendisliği

Sorumlu yazar ve iletişim adresi /Corresponding author and contact address: Ş.M.E.T. / melda.togay@sbu.edu.tr**Müracaat tarihi/Application Date:** 30.10.2021 • **Kabul tarihi/Accepted Date:** 10.12.2021
ORCID IDs of the authors: Ş.M.E.T: 0000-0002-7473-8417; U.T: 0000-0003-0592-9663

Abstract

Objective
This study aims to synthesize and characterize the nanocomposite films incorporating unmodified and modified nanoparticles within the poly(lactic acid) matrix, and to investigate their usage as an alternative scaffold for tissue engineering.

Materials and Methods
Titanium dioxide (TiO_2) nanoparticles were firstly grafted by L-lactic acid oligomer (LA-g-TiO_2) and the mixture of propionic acid/hexylamine (AA-g-TiO_2), respectively. Then the unmodified and modified nanoparticles were incorporated within the poly(lactic acid) matrix via the solvent casting method to produce the PLA/TiO_2, PLA/LA-g-TiO_2, and PLA/AA-g-TiO_2 nanocomposite films. The chemical, thermal and mechanical structures of these synthesized films were subsequently characterized.

Results
The attenuated total reflectance (ATR) results demonstrated that the surface modification of the nanoparticles was accomplished. The results of differential scanning calorimeter (DSC) analysis showed that the crystallization of the PLA was partly increased by the incorporation of modified nanoparticles. The results of thermogravimetric analysis (TGA) showed that the addition of LA-g-TiO_2 into the polymer matrix improved the thermal stability of PLA/LA-g-TiO_2 nanocomposite film more than the addition of AA-g-TiO_2 into the polymer matrix. The first and second decomposition temperatures of the nanocomposites containing LA-g-TiO_2 were 348.3 ^oC and 392 ^oC, respectively, which were 6% greater than those of the neat PLA. The micrograph of atomic force microscopy (AFM) of the nanocomposites indicated that LA-g-TiO_2 and AA-g-TiO_2 were homogeneously dispersed in polymer matrices. The results of dynamic mechanical analysis (DMA) demonstrated that the most efficient bonding and compatibility were obtained in PLA/LA-g-TiO_2 nanocomposite compared to the other nanocomposites.

Conclusion
These grafted nanoparticles, LA-g-TiO_2 and AA-g-TiO_2, enhanced the thermal and mechanical properties of the nanocomposites owing to their uniform distribution in the matrix and good interactions with the polymeric matrix. Therefore, these nanocomposites can be utilized as alternative scaffolds in bone tissue engineering.

Keywords: Poly (lactic acid), Surface modified titanium dioxide, Grafted, Nanocomposite, Nanoparticles, Tissue engineering

Introduction

The demand for tissue engineering has been increased to develop artificial tissues and organs (1) and to cease health problems caused by damaged tissues in recent years. Unfortunately, a lack of finding out functionally suitable and compatible materials is a considerable challenge (2). Therefore, biopolymer-based nanocomposites have attracted more attention in tissue engineering applications (3) due to their high mechanical, biocompatible, and biodegradable properties (4). In general, these nanocomposites can be prepared by the addition of a nanoparticle into a polymer matrix (4). Among a great many biopolymers, poly(lactic acid) (PLA), poly(lactic acid co-glycolic acid) (PLGA), and poly(ε-caprolactone) (PCL) have been widely distinguished in this context (5,6).

PLA can be produced from renewable plant sources, such as corn, beet, starch, and sugar (7, 8). The well-known industrial production method is the ring-opening polymerization of a monomer. Additionally, PLA can be effortlessly formed into a desirable shape, which provides great application areas in the industry (8). It has been widely used in food packaging, textile applications (9), biomedical applications, and controlled drug delivery systems (10,11). Although its processability, biocompatibility, biodegradability, and relatively low-cost properties make it a more promising polymer than the conventional polymers, some limitations related to its low crystallization ability set limits in its applications (8).

The incorporation of nanoparticles within the polymeric matrix has provided unique features, enhanced the structural, biological, thermal properties of these polymers, and yielded the performance of the nanocomposites (7). Therefore, nanocomposites created by the incorporation of nanomaterials into polymers revealed more safe, stable, non-toxic, and sophisticated materials that can be used as an alternative in tissue applications (12).

To create these nanocomposites, carbon nanotubes (13), halloysite nanotubes (14), montmorillonite (15), and titanium dioxide (16), etc. have been often incorporated into polymers. Among these nanoparticles, the most common is titanium

dioxide (TiO_2), which has been approved by the US Food and Drug Administration (FDA) (17). It has great antimicrobial properties, odor inhibition, biocompatibility, inertness, low toxicity, and high antibacterial properties (18).

Recently, owing to its unique antimicrobial activity, cell adhesion, growth properties, polymer, and TiO_2 composite materials have been achieved considerable success in the different fields of tissue engineering (19). Archana et al. produced a wound dressing scaffold by poly(vinylpyrrolidone) (PVP)-chitosan-TiO_2 nanocomposite to recover an open wound in albino rats (20). They proved that approximately 99% of the wound healed up to sixteen days (20). Peng et al. showed that TiO_2-chitosan-collagen nanocomposites completely recovered the wound in animals, and also hair growth was observed in that site (21). In addition to the antimicrobial activity of polymer-TiO_2 composite materials, several experiments have revealed tissue regeneration. Khalid et al. demonstrated that the polymer-TiO_2 nanocomposites enhanced the performance of the bandage by increasing the re-epithelization of damaged tissues of mice (22). Moreover, in another study, high cell attachment was observed on the sites containing TiO_2 nanoparticles of TiO_2-poly(ether-ether-ketone) (PEEK) nanocomposites (23).

In this study, by using two different modification methods, the properties of the nanocomposites including modified nanoparticles were investigated and compared with the nanocomposites including unmodified nanoparticles. To disperse the TiO_2 particles into the PLA matrix without aggregation and improve the property of bioactivity, the surface of the TiO_2 nanoparticles was grafted by using lactic acid with tin chloride as a catalyst and propionic acid with the n-hexylamine solution. The surface grafted TiO_2 nanoparticles were characterized by Attenuated total reflectance (ATR), and the synthesized nanocomposite films were characterized by a Fourier transform infrared spectroscopy (FTIR), differential scanning calorimetry (DSC), thermogravimetric analysis (TGA), atomic force microscopy (AFM), water contact angle analysis, and dynamic mechanical analysis (DMA).

Material and Methods

Materials

Poly(L-lactic acid) with a density of 1.25 g/cm^3 was purchased from Nature Plast (IFS, France). TiO_2 nanoparticles with an average particle size of 25 nm were obtained from Sigma-Aldrich (St. Louis, USA). L-lactic acid (≥98%), propionic acid (≥99.5%), and n-hexylamine (99%) were purchased from Sigma-Aldrich (St. Louis, USA). Tin chloride ($SnCl_2$) was obtained from Carlo Erba (France).

Modification Process

L-Lactic Acid Oligomer

One of the modification processes was performed by the condensation reaction of L-lactic acid with tin chloride ($SnCl_2$) as reported in the literature (5), and it was named LA-g-TiO_2. Briefly, certain amounts of the particles were treated with the tetrahydrofuran solution (25 mL). Then 10 g of L-lactic acid was added dropwise to this mixture and sonicated for 15 min at room temperature to obtain a well-mixed solution. After that, 0.07 g of $SnCl_2$ was added into this mixture as a catalyst (5). When it was warmed up at 160°C for 1.5 h and under vacuum condition at the same temperature by stirring at 200 rpm, the reaction was continued for 6 h. The residual chloroform into the solid was cleaned with distilled water after the precipitates were separated, and the final pellet was dried at 40 ºC under vacuum for 3 days.

Propionic Acid/n-Hexylamine

The other process was performed in the same way as in the previous part. In this procedure, certain amounts of the particles were firstly added to 50 mL of propionic acid (0.1 M) and mixed by magnetically stirring for 24 h. The solution was centrifugated for 15 min, and then the excess acid was removed with ethyl acetate (0.1 M). Certain amounts of methanol were mixed and sonicated for 1 h. Therefore, the dispersion of the precipitation in methanol was achieved. Then 50 mL of n-hexylamine (0.1 M) was mixed and sonicated for 1 h. After the sonication, the precipitation was centrifugated for 15 min, and the excess amount of n-hexylamine was removed by ethyl acetate. Finally, the precipitation, named AA-g-TiO_2, was dried under vacuum at 40 ºC for 3 days.

The Nanocomposite Films

All the nanocomposite films were obtained by a solvent casting method (19,24). At the beginning of the procedure, the PLA and TiO_2 were dried at 80 ºC for 3 h under a vacuum to remove water. 5% (w/v) of PLA was first solved in chloroform, and the mixture was vigorously stirred to dissolve it completely. Subsequently, to produce nanocomposite films, the unmodified and modified nanoparticles were put in this solvent to achieve a nanoparticle weight to solvent ratio of 1% (w/v), and separately dispersed into the polymer mixture. Therefore, the amounts of the polymer and nanoparticle in the films are shown in Table 1. Each solution was sonicated at 25 °C for 4 h and vigorously stirred overnight, and then cast

Table 1 The amounts of the polymer and nanoparticle in the films

Films	PLA (wt.%)	TiO_2 (wt.%)	AA-g-TiO_2 (wt.%)	LA-g-TiO_2 (wt.%)
Neat PLA	5	-	-	-
PLA/TiO_2	5	1	-	-
PLA/AA-g-TiO_2	5	-	1	-
PLA/LA-g-TiO_2	5	-	-	1

onto glass plates and dried for more than 3 days under vacuum oven at 25 ºC to remove the remaining solvent. All the films were kept in a desiccator until used.

Characterizations

The Nanoparticles

Attenuated total reflection spectroscopy (ATR; Bruker Optics Ltd., Coventry, UK) was used to examine the adsorption of organic species on the grafted and non-grafted TiO_2 nanoparticles.

The Nanocomposites

The absorbance of the chemical bonds in the nanoparticles was determined by a Fourier-transform infrared spectroscopy (FT-IR; Nicolet Avatar 370, Thermo Fisher Scientific, Inc., MA, USA) in the range of 4000-400 cm^{-1}.

The thermal properties of the films were determined using a differential scanning calorimeter (DSC; Scinco DSC-N-650, Seoul, Korea). DSC measurements were made with a heating process from 25 to 200 ºC with a scanning rate of 10 ºC/min. The crystallinity of neat polymer and the nanocomposite films was calculated using the following equation (1) (25):

$$X_C(\%) = \left[\frac{\Delta Hm}{93.7}\right] \times 100$$

Where X_c is the crystallinity (%), ΔH_m is the melting enthalpy (J/g), and 100% crystalline of PLA is 93.7 J/g. The thermogravimetric analysis (TGA; TA Instruments Q500, Delaware, USA) was used to determine the amounts of grafted organic materials in the nanocomposite films. All the nanoparticles were measured at 20 ºC/min from room temperature to 900 ºC.

The surface topography of the nanocomposites was determined by atomic force microscopy analysis (AFM; XE-100 AFM Park Systems Corp., Suwon, Korea). The 3D surface topography of the nanocomposite films was taken for 5 × 5 μm^2 at room temperature.

The property of wettability was determined by a water contact angle measurement system with a sessile drop shape analyzer (Krüss DSA 100, Hamburg, Germany). The images were achieved in 10 s at room temperature. The analysis was performed at least three measurements.

The mechanical properties of the nanocomposites were measured using ASTM method D882-12 (ASTM, 2012) with an MTS testing machine (Eden Prairie, MN, USA). The samples (1.27 cm x 10 cm) were put on a grid, and the distance was set at 50 mm at a speed of 5 mm/min.

Results

Characterization of the Nanoparticles

Modification by Lactic Acid

The ATR spectra of neat TiO_2 and LA-g-TiO_2 nanoparticles are given in Figure 1. The non-grafted and grafted TiO_2 nanoparticles displayed the stretching vibration of the Ti-OH group at around 3400 cm^{-1} (5,26). In addition, the Ti-O-Ti linkages were obtained at between 500 and 1000 cm^{-1}, and a weak band at 1620 cm^{-1} was ascribed to adsorbed water (5). In the spectrum of LA-g-TiO_2 nanoparticles, an absorption band of the carbonyl group (C=O) of lactic acid was surprisingly observed at 1760 cm^{-1} due to the surface modification of the neat nanoparticle. The bands at 1500 and 1410 cm^{-1} in the LA-g-TiO_2 nanoparticle were attributed to the asymmetric and symmetric stretching mode of (O-C-O) (27).

Modification by Propionic Acid/n-Hexylamine

The ATR spectra of neat TiO_2 and AA-g-TiO_2 nanoparticles are shown in Figure 1. The peak at about

1620 cm^{-1} and a band between 500 and 1000 cm^{-1} were attributed to the vibration of the Ti-O-Ti linkages in nanoparticles in adsorbed water, respectively (5,24). A carbonyl group (C=O) of propionic acid, the asymmetric and symmetric (COO^-) stretching vibrations were observed at 1760 cm^{-1}, 1550 cm^{-1}, and 1410 cm^{-1}, respectively, in Figure 1. Therefore, the carboxylic group and Ti-OH of the surface of the nanoparticles made a chemical bond (24). The stretching vibration peaks of (NH_2) and (NH_2^+) were seen between 1590-1660 cm^{-1} and 1550-1610 cm^{-1}, respectively.

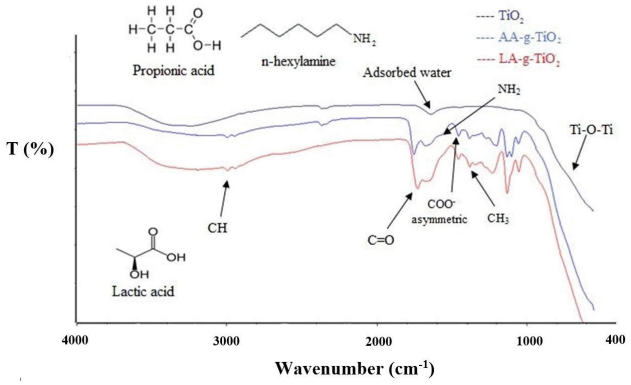

Figure 1:
ATR spectra of (a) neat TiO_2, (b) AA-g-TiO_2 and (c) LA-g-TiO_2

Characterization of the Nanocomposites

FTIR analysis

The FTIR spectra of the films are illustrated in Figure 2. In pure PLA spectrum (Figure 2 (a)), there was a band between 3500 and 3700 cm^{-1} due to -OH stretching vibration, a band between 2900 and 3000 cm^{-1} due to CH stretching, a band at 1760 cm^{-1} due to C=O ester carbonyl stretching, a band between 1350 and 1460 cm^{-1} due to symmetric and asymmetric deformation of CH_3, a band between 1040 and 1270 cm^{-1} due to CO stretching, and a band at 870 cm^{-1} demonstrating C-C stretching vibration (11, 28). When neat PLA and PLA/TiO_2 films were compared, a broad absorption peak at 400-800 cm^{-1} was attributed to the Ti-O-Ti and Ti-O framework bonds in Figure 2 (27).

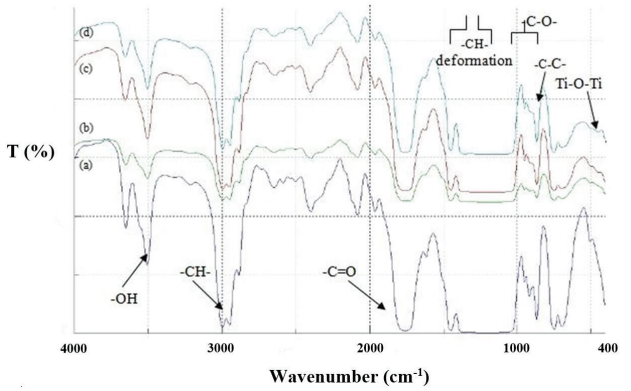

Figure 2:
FTIR spectra of (a) neat PLA (b) PLA/TiO_2 (c) PLA/AA-g-TiO_2 (d) PLA/LA-g-TiO_2

Thermal Properties

The results of the thermal properties of the films are shown in Table 2. The addition of the grafted TiO_2 into the polymer matrix did not result in a remarkable shift in the glass transition temperature (Tg) value when compared with the neat PLA. However, there had been a decrease in this value from 73.70 ºC to 59.43 ºC with the non-grafted nanoparticles into the film. The addition of the non-grafted TiO_2 and grafted TiO_2 nanoparticles improved the crystallinity of the films.

In addition, the decomposition temperatures of the films are depicted in Table 3. The incorporation of the nanoparticles in the PLA/TiO_2 nanocomposites, the first decomposition temperature slightly changed to higher temperatures. The PLA/TiO_2, PLA/LA-g-TiO_2, and PLA/AA-g-TiO_2 nanocomposites had higher first decomposition temperatures (334.89, 331.84, and 348.30 ºC, respectively) than the neat PLA that had the first decomposition temperature at 328.91 ºC.

AFM Analysis

The topological features of the films are investigated by AFM as shown in Figure 3 and the results of the surface roughness of the films are given in Table 4. The AFM result depicts a flat surface morphology for the neat PLA film in Figure 3(a). In the non-grafted TiO_2 and PLA nanocomposite films (Figure 3(b)), the

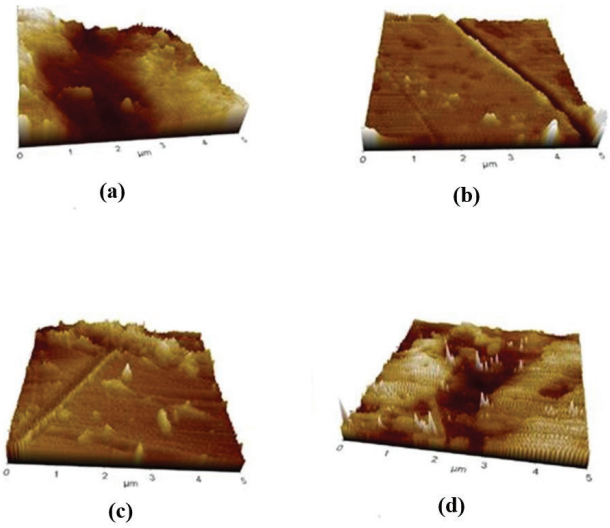

Figure 3:
3D surface topography of (a) neat PLA, (b) PLA/TiO_2, (c) PLA/AA-g-TiO_2 and (d) PLA/LA-g-TiO_2

Table 2 Thermal and crystalline properties of the films

Films	Glass Transition Temperature (T_g, °C)	Melting Temperature (T_m,°C)	Melting Enthalpy (ΔH_m, J/g)	Crystallinity (X_c, %)
Neat PLA	73.70	149.12	28.30	30.20
PLA/ TiO_2	59.43	142.70	40.90	43.64
PLA/AA-g-TiO_2	73.41	148.51	29.90	31.91
PLA/LA-g-TiO_2	75.57	150.05	34.34	36.65

Table 3 The decomposition temperatures of the films

Films	First decomposition temp.(°C)	Second decomposition temp. (°C)	Residue (%) (at 800 °C)
Neat PLA	328.91	370.28	1.635
PLA/TiO_2	334.89	372.82	1.770
PLA/AA-g-TiO_2	331.84	364.20	2.304
PLA/LA-g-TiO_2	348.30	392.00	0.698

Table 4 The surface roughness of the films

Films	Surface Roughness (nm)
Neat PLA	0.179
PLA/TiO_2	0.021
PLA/AA-g-TiO_2	0.255
PLA/LA-g-TiO_2	0.604

Table 5 Water contact angles on the surfaces of the films

Films	Contact angle, q, (STD) [deg.]
Neat PLA	82.6 (±6.7)
PLA/TiO_2	69.3 (±1.1)
PLA/AA-g-TiO_2	72.1 (±4.6)
PLA/LA-g-TiO_2	74.0 (±5.5)

aggregation of the non-grafted TiO_2 nanoparticles clearly emerged on the surface of the nanocomposites. However, in the case of the AA-g-TiO_2 nanoparticles, there was a uniform dispersion of the nanoparticles into the matrices without aggregation in Figure 3(c). Moreover, in the case of the LA-g-TiO_2 nanoparticles, the best dispensability in the PLA matrix is illustrated in Figure 3(d).

Water Contact Angle Analysis

The contact angle of the films is listed in Table 5. It is exactly known that the water contact angle measures the hydrophilicity of surfaces. When the surface modification with the ionizable groups is applied, the water contact angle decreases due to the facile hydrogen bonding between the ionizable groups and water molecules (29). As the comparison between the average contact angle of the neat PLA matrix and the nanocomposites including non-modified/modified TiO_2, the average contact angles decreased as shown in Table 5.

Hydroxyl groups on the TiO_2 surface reduce the surface contact angle, which was illustrated in Figure 4. Especially the contact angles of the nanocomposite films which contained TiO_2, LA-g-TiO_2, and AA-g-TiO_2 nanoparticles shifted to low values (69.3°, 74.0°, and 72.1°, respectively) when compared to the neat PLA (82.6°).

Mechanical Properties

It is well-known that materials give a response to a mechanical force, which is a function of the

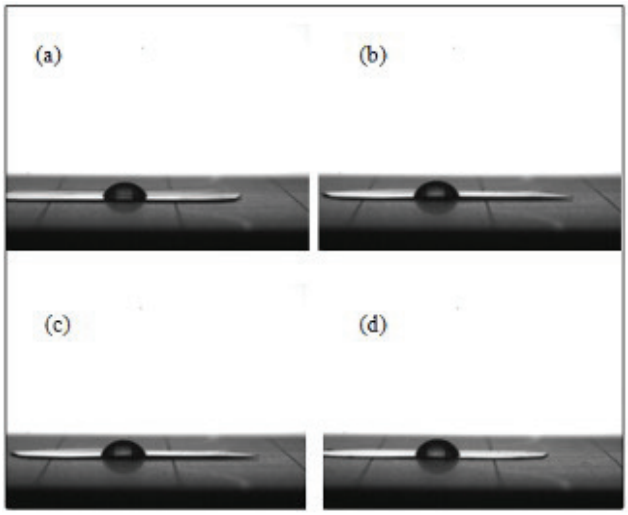

Figure 4:
Water contact angle images of (b) neat PLA, (b) PLA/TiO_2, (c) PLA/AA-g-TiO_2, (d) PLA/LA-g-TiO_2

temperature. This response is composed of the storage modulus (E'), the loss modulus (E''), and tan δ, which is the E''/ E' ratio (30), as shown in Figure 5. The shifts in tan δ to higher temperatures for the nanocomposite materials suggest the increasing adhesion between the polymer and the reinforcement in the system (31). In this study, the presence of the non-grafted and grafted TiO_2 nanoparticles showed a considerable shift and expansion of the tan δ curves for all the nanocomposites compared to that of the neat PLA. It was attributed to the limited motions of the polymer chains by the inorganic network. Especially,

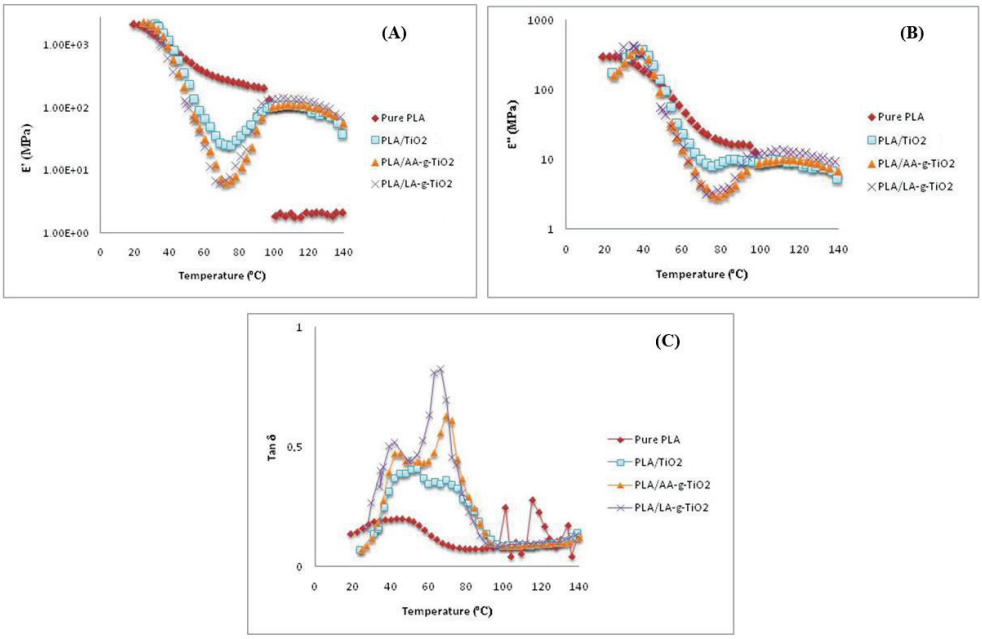

Figure 5:
(A) Storage modulus, (B) Loss modulus, and (C) Variation of the tan δ with temperature of the films

PLA/LA-g-TiO_2 nanocomposites exhibited a sharp increment for tan δ and intensity. Therefore, the most efficient bonding and compatibility were obtained by the PLA/LA-g-TiO_2 nanocomposite film compared to the other nanocomposite films.

Discussion

PLA-based composite materials have been extensively used in tissue engineering and controlled release fields due to their excellent biocompatibility, biodegradability, and processability (12). As a synthetic polymer, PLA lacks the adequate mechanical strength essential for bone tissue engineering applications, and hence various approaches for improvements of its property have been carried out involving structural modification, blending polymers, and incorporation of nanoparticles to form nanocomposites (18). In this study, unmodified and modified nano-TiO_2 particles were incorporated into PLA bulk to improve its mechanical behavior.

Two different modification methods were performed by grafting the surface of the TiO_2 nanoparticles by using lactic acid with tin chloride as a catalyst (LA-g-TiO_2), and propionic acid with the n-hexylamine solution (AA-g-TiO_2). It has been reported by Luo et al. (27) that the asymmetric and symmetric stretching mode of (O-C-O) were observed at 1500 and 1410 cm^{-1} in the LA-g-TiO_2 nanoparticle when the lactic acid oligomer was successfully grafted on the nanoparticles. On the other side, when the spectrums of TiO_2 and the AA-g-TiO_2 nanoparticles were compared, the new bands at 1000-1150 cm^{-1} belonging to C-O-C and C-CH_3 were exactly apparent (26). Therefore, this was achieved by infusing the nanoparticles with propionic acid and n-hexylamine. Moreover, Nakayama et al. (24) explained that the stretching vibration peaks of (NH_2) and (NH_2^+) observed between 1590-1660 cm^{-1} and 1550-1610 cm^{-1} overlapped.

Solvent casting method was used to manufacture PLA/AA-g-TiO_2 and PLA/LA-g-TiO_2 nanocomposite films. The incorporation of the grafted nanoparticles within PLA for PLA/AA-g-TiO_2 and PLA/LA-g-TiO_2 nanocomposite films showed that Ti-O-Ti and Ti-O framework bonds were obtained at the same wavenumber as PLA/TiO_2 nanocomposite films (27).

Differential scanning calorimeter (DSC) analysis showed that a decrease in the melting temperatures (Tm) for all the nanocomposite films pointed out a decline of the mass of the lamellar phase of the polymer owing to the nanoparticles (27). After the addition of nanoparticles, the crystallinity of the films increased due to the distribution of the chain regularity, and also the crystallization becomes easier with the chemical bond between the nanoparticles and the polymer chain (32). Similar results were obtained in the studies on PLA/TiO_2 nanocomposites, studied by Athanasoulia et al. and Nomai et al. (32, 33). Due to the limited thermal motion of PLA in the nanoparticles network, the addition of a small number of nanoparticles increases the remaining loading of the nanocomposites (25). The results of thermogravimetric analysis (TGA) showed that the addition of LA-g-TiO_2 into the polymer matrix improved the thermal stability of PLA/LA-g-TiO_2 nanocomposite film more than the addition of AA-g-TiO_2 into the polymer matrix. Generally, the addition of the non-grafted and grafted TiO_2 nanoparticles into the PLA increased the residual weight of the nanocomposites at a high temperature (at 800 ºC).

During the analysis of the topological features of the films, a uniform dispersion of the nanoparticles into the matrices without aggregation were observed with increasing the surface roughness. A similar result was reported by Buzarovska that the incorporation of TiO_2 into the polymer matrix increased the surface roughness (34). Additionally, it is exactly known that while the non-grafted TiO_2 nanoparticles were completely precipitated, the grafted nanoparticles, both AA-g-TiO_2 and LA-g-TiO_2, were easily mixed in chloroform, and a uniform suspension was obtained. In other nanocomposite films, there were parallel outcomes reached by Bodaghi et al. and Li et al. (17, 18).

It is exactly known that the addition of TiO_2 reduced the surface contact angle owing to its hydroxyl groups (35). This result demonstrates that a hydrophilic surface for PLA nanocomposites can be obtained by adding TiO_2 nanoparticles. The results of dynamic mechanical analysis (DMA) showed that the most efficient bonding and compatibility were obtained in PLA/LA-g-TiO_2 nanocomposite compared to the other nanocomposites.

Conclusion

The modification of the nanoparticles was successfully achieved by grafting L-lactic acid oligomer and propionic acid/hexylamine on the surface of TiO_2 nanoparticles named LA-g-TiO_2 and AA-g-TiO_2, respectively. Then the solvent casting method was employed to prepare the nanocomposites containing non-grafted and grafted TiO_2 nanoparticles. The grafted nanoparticles were uniformly dispersed into the matrices without aggregation. The uniformed

PLA/LA-g-TiO_2 and PLA/AA-g-TiO_2 nanocomposite films demonstrated that the thermal and mechanical properties of these materials increased when compared to the neat PLA and PLA/TiO_2 due to the homogeneous distribution of the grafted TiO_2 nanoparticles in the polymer matrix. Therefore, the interfacial combination between the grafted TiO_2 nanoparticles and the polymer matrix was achieved. The prepared PLA/LA-g-TiO_2 and PLA/AA-g-TiO_2 nanocomposites can be potential scaffolds for bone tissue engineering.

Acknowledgment
The authors express their sincere appreciation to Prof. Dr. Nursel DİLSİZ for her help.

Conflict of Interest Statement
The authors have no conflicts of interest to declare.

Ethical Approval
This research does not contain any studies with human or animal subjects.

Funding
This research was supported by the Gazi University Scientific Research Projects Unit [grant number BAP 06/2012-03].

Author Contributions
ŞMTE: Data curation; Investigation; Methodology; Visualization; Writing-original draft, Writing-review & editing.

UT: Conceptualization; Formal analysis; Investigation; Validation; Writing-original draft.

References

1. Khademhosseini A, Langer R. A decade of progress in tissue engineering. Nature Protocols 2016; 11(10): 1775-81.
2. Ghosal K, Agatemor C, Spitalsky Z, Thomas S, Kny E. Electrospinning tissue engineering and wound dressing scaffolds from polymer-titanium dioxide nanocomposites. Chemical Engineering Journal 2019; 358: 1262-78.
3. Saber-Samandari S, Yekta H, Ahmadi S, Alamara K. The role of titanium dioxide on the morphology, microstructure, and bioactivity of grafted cellulose/hydroxyapatite nanocomposites for a potential application in bone repair. International Journal of Biological Macromolecules 2018; 106: 481-8.
4. Rajeshwari V, Fernando J. Poly paraphenylene diamine/titanium dioxide/exfoliated graphite nanocomposites: Synthesis and characterisation. Materials Today 2021; Proceedings, In press.
5. Lu X, Lv X, Sun Z, Zheng Y. Nanocomposites of poly(l-lactide) and surface-grafted TiO2 nanoparticles: Synthesis and characterization. European Polymer Journal 2008; 44(8): 2476-81.
6. Wang Y, Dai J, Zhang Q, Xiao Y, Lang M. Improved mechanical properties of hydroxyapatite/poly(ε-caprolactone) scaffolds by surface modification of hydroxyapatite. Applied Surface Science 2010; 256(20): 6107-12.
7. Shebi A, Lisa S. Evaluation of biocompatibility and bactericidal activity of hierarchically porous PLA-TiO2 nanocomposite films fabricated by breath-figure method. Materials Chemistry and Physics 2019; 230: 308-18.
8. Fonseca C, Ochoa A, Ulloa MT, Alvarez E, Canales D, Zapata PA. Poly(lactic acid)/TiO2 nanocomposites as alternative biocidal and antifungal materials. Material Science and Engineering C 2015; 57: 314-20.
9. De Silva RT, Pasbakhsh P, Lee SM, Kit AY. ZnO deposited/encapsulated halloysite-poly (lactic acid) (PLA) nanocomposites for high performance packaging films with improved mechanical and antimicrobial properties. Applied Clay Science 2015; 111: 10-20.
10. Battistella E, Varoni E, Cochis A, Palazzo B, Rimondini L. Degradable polymers may improve dental practice. Journal of Applied Biomaterials and Biomechanics 2011; 9(3): 223-31.
11. Salahuddin N, Abdelwahab M, Gaber M, Elneanaey S. Synthesis and Design of Norfloxacin drug delivery system based on PLA/TiO2 nanocomposites: Antibacterial and antitumor activities. Material Science and Engineering C 2020; 108: 110337.
12. Bharadwaz A, Jayasuriya AC. Recent trends in the application of widely used natural and synthetic polymer nanocomposites in bone tissue regeneration. Materials Science and Engineering: C 2020; 110: 110698.
13. Chen C, He BX, Wang SL, Yuan GP, Zhang L. Unexpected observation of highly thermostable transcrystallinity of poly(lactic acid) induced by aligned carbon nanotubes. European Polymer Journal 2015; 63: 177-85.
14. De Silva RT, Pasbakhsh P, Goh KL, Mishnaevsky L. 3-D computational model of poly (lactic acid)/halloysite nanocomposites: Predicting elastic properties and stress analysis. Polymer 2014; 55: 6418-25.
15. Pluta M, Jeszka JK, Boiteux G. Polylactide/montmorillonite nanocomposites: Structure, dielectric, viscoelastic and thermal properties. European Polymer Journal 2007; 43(7): 2819-35.
16. Zapata PA, Palza H, Delgado K, Rabagliati FM. Novel antimicrobial polyethylene composites prepared by metallocenic in situ polymerization with TiO2-based nanoparticles. Journal of Polymer Science Part A: Polymer Chemistry 2012; 50(19): 4055-62.
17. Bodaghi H, Mostofi Y, Oromiehie A, Zamani Z, Ghanbarzadeh B, Costa C, Conte A, Del Nobile MA. Evaluation of the photocatalytic antimicrobial effects of a TiO2 nanocomposite food packaging film by in vitro and in vivo tests. LWT - Food Science and Technology 2013; 50(2): 702-6.
18. Li S, Chen G, Qiang S, Yin Z, Zhang Z, Chen Y. Synthesis and evaluation of highly dispersible and efficient photocatalytic TiO2/poly lactic acid nanocomposite films via sol-gel and casting processes. Internation Journal of Food Microbiology 2020; 331: 1087663.
19. Baek N, Kim YT, Marcy JE, Duncan SE, O'Keefe SF. Physical properties of nanocomposite polylactic acid films prepared with oleic acid modified titanium dioxide. Food Packaging and Shelf Life 2018; 17: 30-38.
20. Archana D, Dutta J, Dutta PK. Evaluation of chitosan nano dressing for wound healing: characterization, in vitro and in vivo studies. International Journal of Biological Macromolecules 2013; 57: 193-203.
21. Peng CC, Yang MH, Chiu WT, Chiu CH, Yang CS, Chen YW et al. Composite nano-titanium oxide-chitosan artificial skin exhibits strong wound-healing effect-an approach with anti-inflammatory and bactericidal kinetics. Macromolecular Bioscience 2008; 8: 316–27.
22. Khalid A, Ullah H, Ul-Islam M, Khan R, Khan S, Ahmad F et al. Bacterial cellulose–TiO2 nanocomposites promote healing and tissue regeneration in burn mice model. RSC Advances 2017; 75: 47662-8.
23. Wu X, Liu X, Wei J, Ma J, Deng F, Wei S. Nano-TiO2/PEEK bioactive composite as a bone substitute material: in vitro and in vivo studies. International Journal of Nanomedicine 2012; 7: 1215-25

24. Nakayama N, Hayashi T. Preparation and characterization of poly(l-lactic acid)/TiO2 nanoparticle nanocomposite films with high transparency and efficient photodegradability. Polymer Degradation and Stability 2007; 92(7): 1255-64.
25. Yan S, Yin J, Yang Y, Dai Z, Ma J, Chen X. Surface-grafted silica linked with l-lactic acid oligomer: A novel nanofiller to improve the performance of biodegradable poly(l-lactide), Polymer 2007; 48(6): 1688-94.
26. Luo YB, Wang XL, Xu DY, Wang YZ. Preparation and characterization of poly(lactic acid)-grafted TiO2 nanoparticles with improved dispersions. Applied Surface Science 2009; 255(15): 6795–6801.
27. Luo YB, Li WD, Wang XL, Xu DY, Wang YZ. Preparation and properties of nanocomposites based on poly(lactic acid) and functionalized TiO2, Acta Materialia 2009; 57(11): 3182-91.
28. Bae GY, Jang J, Jeong YG, Lyoo WS, Min BG. Superhydrophobic PLA fabrics prepared by UV photo-grafting of hydrophobic silica particles possessing vinyl groups. Journal of Colloid and Interface Science 2010; 344(2): 584-7.
29. Athanasoulia IGI, Tarantili PA. Thermal transitions and stability of melt mixed TiO2/Poly(L-lactic acid) nanocomposites. Polymer Engineering Science 2019; 59: 704-13.
30. Nomai J, Suksut B, Schlarb AK. Crystallization Behavior of Poly(lactic acid)/Titanium Dioxide Nanocomposites. KMUTNB International Journal of Applied Science and Technology 2015; 8(4): 1-8.
31. Buzarovska A. PLA Nanocomposites with Functionalized TiO2 Nanoparticles. Polymer-Plastics Technology and Engineering 2013; 52(3): 280-6.
32. Goddard JM, Hotchkiss JH. Polymer surface modification for the attachment of bioactive compounds. Progress in Polymer Science 2007; 32(7): 698-725.
33. Wu CY, Tu KJ, Deng JP, Lo YS, Wu CH. Markedly enhanced surface hydroxyl groups of TiO2 nanoparticles with superior water-dispersibility for photocatalysis. Materials (Basel) 2017; 10(5): 566-71.
34. Sinha Ray S, Yamada K, Okamoto M, Ueda K. New polylactide-layered silicate nanocomposites. 2. Concurrent improvements of material properties, biodegradability and melt rheology. Polymer 2003; 44: 857-66.
35. Wu CS, Liao HT. Study on the preparation and characterization of biodegradable polylactide/multi-walled carbon nanotubes nanocomposites. Polymer 2007; 48(15): 4449-58